

Stimulus-driven Coordination of Cortical Cell Assemblies and Propagation of Gestalt Belief in V1

Yves Frégnac, Pedro V. Carelli,
Marc Pananceau, and Cyril Monier

Abstract

This chapter reviews the concept of dynamic coordination in the mammalian primary sensory cortex during low-level (non-attention-related) perception. Among critical issues, it questions the necessity to keep the relational information (the “whole”) separable from the information carried initially by each stimulus component (the “parts”). It also underlines the need for documenting in higher mammals the possible existence of subcortical or cortical supervisors, whose firing activation or suppression would condition the merging and segmentation of functional cortical assemblies. Emphasis is given to cases where coordination is generated by the sensory drive itself and amplified by built-in anisotropies in the network connectivity. The joint comparison of synaptic functional imaging (at the intracellular level) and real-time voltage-sensitive dye network imaging (at the functional map level) is used to demonstrate the role of intracortical depolarizing waves, broadcasting an elementary form of collective belief. The functional features of these slow waves support the hypothesis of a dynamic association field, propagating synaptic modulation in space and time through lateral (and possibly feedback) connectivity, which accounts for the emergence of illusory motion percepts predicted by the Gestalt theory.

For a Taxonomy of Dynamic Coordination

Coordination of distributed elementary dynamic processes into a coherent “whole” is the organizational hallmark of brain cognitive activity. Dynamic coordination is required so that, by using time as an additional coding dimension, the “whole” can be distinguished from the “static” sum of the parts. Failure to do so results in superposition catastrophe (von der Malsburg 1986).

Flexibility in coordination ability is necessary so that the functional outcome of the ensemble remains adapted to the ever-changing goals which govern relationships between the “self” and the “outer” world.

Historically, dynamic reconfiguration of neural activities has been considered by many explorers of the brain—philosophers, psychologists, and physiologists—as a likely substrate for thoughts, dreams, and other mental processes, with particular relevance to perception and memory recall. Without much knowledge of the circuits involved, and inspired by the brilliant concept of cell assemblies introduced by Yves Delage (1919) and Donald Hebb (1949; reviewed in Frégnac 2002), theoreticians of the brain later imagined the waxing and waning of synchronized oscillations or synfire chains as the dynamic signature of coordination (Milner 1974; von der Malsburg 1981/1994; Abeles 1982). As beautifully worded by Delage (1919), the concept of “parasynchronization” implies that “every modification engraved in the neuron’s vibratory mode as a result of its co-action with others leaves a trace that is more or less permanent in the vibratory mode resulting from its hereditary structure and from the effects of its previous co-actions. Thus its current vibratory mode reflects the entire history of its previous participations in diverse representations.” It is therefore not surprising that numerous contemporaneous brain scientists, under the flagship of Wolf Singer and Christoph von der Malsburg, recognize the fugitive emergence of associative percepts in the gamma wave signature of V1 local field potentials (Fries 2009; Tallon-Baudry, this volume).

In its simplest form, dynamic coordination is defined by the multiple interrelations in space and time that can be drawn between elements of any given assembly. Its phenomenological expression is signaled by the reconfiguration of elementary dynamics and their potential phase relations as a function of an externally defined context or an internally generated goal. Phillips et al. (this volume) constrain the issue further by adding: “in general, coordinating interactions are those that produce coherent and relevant overall patterns of activity, while preserving the essential individual entities and functions of the activities coordinated.” This additional constraint implies that the dynamic binding process itself should not interfere with local properties of the interlinked elements (which these authors refer to as “meaning” tokens). This hypothesis has its own virtue since numerous cognitive operations seem to preserve at the same time the representation of the “parts” (segmentation) and the “whole” (binding). In sensory perception, this applies to vision, where fusion and perception coexist together, and to a certain extent to audition, but probably less to olfaction. In this latter case, the perception of the “whole” overrides that of each component, especially when the subject is given heteromodality priors (e.g., the “color” of smell in oenology; Morrot et al. 2001). At a more abstract level, such condition is needed in the compositionality framework set by Fodor and Pylyshyn (1988), where elementary features have a fixed symbolic value (a letter in an alphabet). In the conceptual view defended by Bill Phillips, compositionality operates as a relational grammar which does not interfere with

the semantic value of the elements. However, there is no strong reason for reducing dynamic coordination in neural systems to linguistic compositionality, although abstract models of logogenesis have been proposed where the brain composes language from the fast reversible binding of synfire chains (Doursat 1991; Bienenstock 1996).

The obvious, critical issue that should be discussed is that coordination or “binding” in the brain operates not between fixed entities called “neurons” but rather between local dynamic integrative processes, each being specific to the considered “neuron.” In classical *in vitro* electrophysiological studies, neurons have an identification profile that is empirically defined at three levels: (a) morphological/structural identity, (b) excitability spiking pattern in response to intracellularly injected current (a kind of crude input/output curve) which characterizes the intrinsic conductance repertoire, and (c) genomic expression pattern revealed by multiplex PCR of the cytoplasmic content (Toledo-Rodriguez et al. 2004; Markram 2006; reviewed in Frégnac et al. 2006). In sensory cortical networks, the elementary neuronal integrative function is also characterized *in vivo* by a static receptive field organization (equivalent to a stimulus/response curve). The discharge field organization revealed by impulse-like sensory stimulus is largely dominated by the convergence patterns of labeled lines extrinsic to the studied structure (for V1, coming from the dorsal lateral geniculate nucleus, LGNd, in the thalamus). The strict application of Bill Phillips’ criteria, as present in many of the early pioneering experiments by Wolf Singer’s team (e.g., Gray et al. 1989; Kreiter and Singer 1996), would suggest that the processing realized by each neuron on elementary parts of the composite stimulus reflects fixed discharge field properties and remains unchanged during associative center-surround stimulation protocols. The underlying assumption is that the relational information should remain separable from the information carried initially by each stimulus component taken in isolation.

To debate this issue further, let us turn from the literature of mammalian cortex to that of invertebrate sensorimotor ganglion: the particular case of the stomatogastric ganglion of the lobster constitutes a striking example of assembly dynamic reconfiguration correlated with changes in behavior where, during the coordination, the electrical input/output properties of individual elements are not preserved. This paucineuronal net is an assembly of giant cells with invariant morphology, and their number is limited enough such that the total blockade of the afferent connectivity to any given cell can be obtained by photo-inactivating all the putative synaptic partners. Early experiments in the invertebrate revealed that isolated neurons are, in all cases, conditional oscillators, displaying a large variety of intrinsic membrane potential patterns such as bursting, plateau, postinhibitory rebound, and spike-frequency adaptation. Further work showed that the repertoire of intrinsic conductances dramatically changes in the presence of neuromodulatory signals secreted by specific broadcasting units in the afferent sensory network (Dickinson and

Nagy 1983). These cells play the role of “orchestra leaders” whose activity triggers the widespread diffusion of neuromodulators. This neuromodulation impacts on the intrinsic reactivity of the other cells by changing reversibly the expressed repertoire of membrane conductances. Consequently, the individual excitability patterns of any given cell will change depending on the context (before, during, or after the orchestra leader cell has fired). This flexibility in intrinsic properties explains why switching on and off neuromodulation reorganizes the dynamics of the full network in distinct functional central motor program generator assemblies, each associated with different motor behaviors, such as swallowing, crunching in the gastric bag, expulsion of processed food for the considered example (Hooper and Moulins 1989; Dickinson et al. 1990; Meyrand et al. 1991) (see Figure 12.1). In this paucineuronal biological network, where all partners are known, the coordinator is identified and the causal link between the temporal assembly motifs and the behavioral actions as well as their functional significance are clearly defined.

These data, often ignored from the vertebrate neuroscience community, support the hypothesis of the existence of “orchestra leader”-like neurons which, through the presence or absence of firing activity, condition and format merging and segmentation across functional assemblies. The existence of giant identified coordinators with invariant morphology and widespread projections has been confirmed in other invertebrate species and, in the bee, associated with reward; however, evidence in larger central networks, such as the mammalian brain, is still lacking. Nevertheless, there is already ample evidence that aminergic and cholinergic subcortical brainstem nuclei release neuromodulator *en passant* along their long axonal projections that travel through all cortical areas, from the occipital to the frontal lobe, and change the repertoire of expressed conductances. Like central pattern generators, thalamic circuits are subject to neuromodulatory influences (Steriade 1996). In this case, neuromodulators, such as acetylcholine, norepinephrine, or serotonin, affect intrinsic currents and switch the circuit from an oscillatory mode to a “relay mode” in which oscillations are abolished (McCormick 1992). These neuromodulators are present in activated states, promoting the relay of sensory information by the thalamus, while their diminished levels during slow-wave sleep unmask participation by the thalamus in the genesis of large-scale synchronized oscillations involving the entire thalamocortical system. We conclude from this brief review that, to a certain extent, both in invertebrate ganglia and the vertebrate brain, the dogma of separability between intrinsic and extrinsic factors in the control of cellular excitability is doomed to fail. Thus, the “whole” cannot be the sum of the “parts,” and segmentation does not always coexist with perceptual binding.

Other examples can be considered where the coordinating agent is not part of the biological system but rather the product of high-order statistical features present in the sensory input stream. Changing the statistical regularities of the environment produces a drastic reorganization of ensemble activity patterns

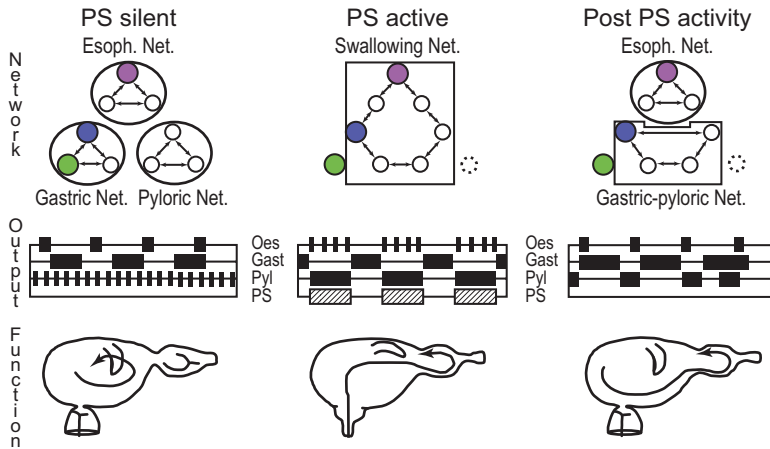


Figure 12.1 Example of dynamic coordination: Reconfiguration of network dynamics by internal “orchestra leaders” in the stomatogastric ganglion of the lobster. The same sensorimotor network is functionally reorganized in independent assemblies depending of the activity state of neuromodulating cells (PS cell) (top row). These assemblies are characterized by specific excitability patterns expressed by each of the composing cells and specific phase relationships between them (middle row). The functional role of each assembly during the swallowing stomatogastric cycle is depicted (bottom row). When PS is silent, the esophageal, gastric, and pyloric networks (top) generate independent rhythmic output patterns (middle) involved in regionally specific and separate behavioral tasks (bottom). When PS is rhythmically active, it drives the opening of the esophageal valve (bottom), and by disrupting the preexisting network(s) and recruiting only part of the neurons, it constructs a novel assembly (top) that generates a coordinated motor pattern (middle) appropriate for swallowing behavior. When PS is again silent post-activity, the esophageal valve closes (bottom) and motor units immediately resume their original network activity while units (i.e., gastric and pyloric) controlling regions more caudal to the sphincter continue to generate a single pattern before resuming their separate activities (adapted from Meyrand et al. 1991). Note that the same cell (color coded) can switch from assembly to the next; this dynamic reconfigurability accounts for behavioral changes.

and their stimulus-locked reliability in the early visual system of mammals. For instance, the presentation of drifting gratings in a V1 receptive field (Figure 12.2) evokes dense but highly unreliable responses across individual trials, both at the spiking and subthreshold levels. In contrast, virtual eye-movement animation of natural scenes temporally evokes in the same cell precise sparse spike responses and stimulus-locked membrane potential dynamics, which are highly reproducible from one trial to the next (Frégnac et al. 2005; Marre et al. 2005; Baudot et al., submitted). Importantly, the fast components of the membrane potential trajectory show a high trial-to-trial reproducibility, even when the cell is not firing, for silent periods extending for several hundred of milliseconds prior and after the reliable spiking event (Figure 12.2).

From "Dynamic Coordination in the Brain: From Neurons to Mind,"

C. von der Malsburg, W. A. Phillips, and W. Singer, eds. 2010. Strüngmann Forum Report, vol. 5, series ed. J. Lupp. Cambridge, MA: MIT Press. ISBN 978-0-262-01471-7.

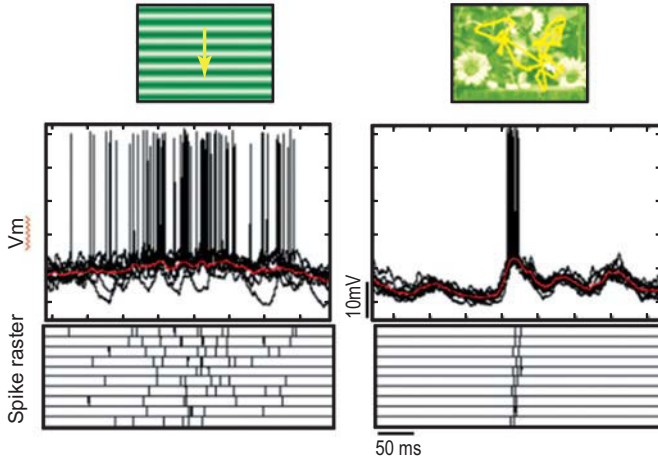


Figure 12.2 Example of dynamic coordination: Coordination by the statistics of the sensory drive. Reconfiguration of spike timing precision as a function of input statistics (adapted from Frégnac et al. 2005). The left and right panels represent evoked sub-threshold (top) and spiking activity patterns (bottom), evoked in the same V1 cell, respectively, for a drifting grating and a natural scene animation. Trial-by-trial membrane potential trajectories are overlaid in black; red indicates mean Vm response. The raster dot displays of the spiking activity are built on ten trials. All records are synchronized with the stimulus onset, and the visualization window is adjusted to illustrate a time period in the movie where evoked spikes are observed. The response of the same cell is dense and noisy for the grating, whereas it is sparse and highly reliable from trial-to-trial for the natural scene.

In this second example, coordination is unrelated to the behavioral outcome driven by perception or neuromodulation, since it is observed in the anesthetized and paralyzed preparation (Frégnac et al. 2005) as well as in the attentive-behaving monkey (Vinje and Gallant 2000). Stimulus-driven recruitment of dynamic nonlinearities distributed across the network results in the sparsening and reordering of spiking events. This self-organized process adapts the temporal precision of the sensory code to the statistics of the input (for further definitions of self-organized coordination, see Engel et al., this volume). The more complex or the closer to a natural environment the input is, the higher the temporal precision of stimulus-locked events are and the more deterministic-like the network dynamics behave. However, and in contrast with the first example, this adaptive form of temporal coordination is done in the absence of an internal executive or supervision units. Multiscale cooperation across the network is still needed, and long distance center-surround interactions across the visual field—which implies long-distance interactions across the retinotopic cortical map—suppress or facilitate interneuronal binding. Note also that, as demonstrated in the first example, the full field stimulation (i.e., “whole” condition) will affect *in fine* the functional characteristics of the recorded unit (i.e., the individual receptive fields of the V1 cells). The classical discharge field defined

with low dimensionality stimuli (Fourier input, sinusoidal luminance grating) does not predict, at least in our hands, the subthreshold dynamical responses of the same cell stimulated with richer input statistics (temporal modulation reproducing eye-movement effects, spatial $1/f^n$ spectrum for natural scenes).

A third class of examples focuses on relational coding in cortex. Long-duration single-frequency tones do not evoke tonic changes in the firing rate of single neurons in auditory cortex. At most, transient burst responses are detected in A1 cortex, at the onset or offset of the tone. The presence of the stimulus, however, is signaled in the same area by a dramatic and tonic elevation in the correlation between cortical units coding for the sound frequency, without any apparent change of firing rate (deCharms and Merzenich 1996). Figure 12.3 illustrates the case where the information that can be stored or recalled on the basis of coordinated activity is separable from the rate responses of single neurons. Furthermore, the cortical domains of shared activation can be expanded or contracted through the coordinating action of a neuromodulator (acetylcholine) or by stimulating the ascending afferent cholinergic corticofugal projection from the nucleus basalis (Kilgard and Merzenich 1988).

A fourth example of coordination, partially of the same class, can be revealed by stimulus-locked analysis of the covariation of the firing rates of several simultaneously recorded units in premotor cortex of awake animals

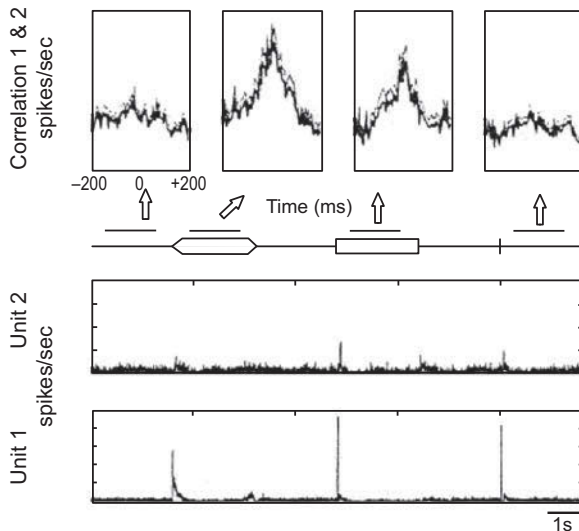


Figure 12.3 Example of dynamic coordination: Reconfiguration of synchrony during sensory processing (adapted from deCharms and Merzenich 1996). A1 cortical units have been simultaneously recorded during a sequence alternating control (silent) and stimulation periods with different tones and temporal profiles. Bottom: PSTHs show fast transient responses in the evoked mode for the onset and offset of the tones, but no tonic activity. Top: Correlograms show decorrelation between units in the ongoing mode and tonic coordination maintained as long as the tone is present.

submitted to a GO/NO-GO paradigm (Figure 12.4). The computation of the time course of the joint activity between units gives access to the dynamics of effective connectivity between simultaneously recorded units (Aertsen et al. 1989). This calculus requires the averaging of joint peristimulus time histograms (PSTHs) over trials corresponding to the same behavioral task (GO vs. NO-GO). The remarkable result is that the stimulus-locked time course of the effective connectivity is flexible and differs significantly between the two task phases (Vaadia et al. 1995). This implies that some task-related coordination switches the functional allegiance of the two recorded neurons between two different relational assemblies. Again, in this example, the rate mean of each unit is unchanged whereas the rate covariation signals information related to the behavioral significance of the cognitive task (GO vs. NO-GO).

These examples of dynamic coordination show a diversity of processes where the coordinating agent can take several forms: in Figure 12.1 and 12.4 it is an internal supervisor embedded in the network; in Figure 12.2 and 12.3 it is the sensory drive or, in Figure 12.4, an external prior. Other examples could have been given where the coordinator is generated by the correlations

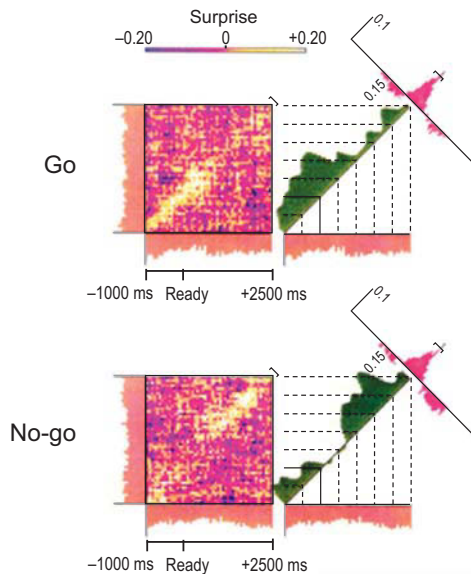


Figure 12.4 Example of dynamic coordination: Reconfiguration of effective connectivity during operant conditioning GO/NO-GO paradigm (adapted from Vaadia et al. 1995). Effective connectivity between simultaneously recorded cortical units is measured by joint PSTHs and statistical surprise measure matrix. The time profile of the synchrony level (green) between the two simultaneously recorded units is represented as a function of delay from trial onset, respectively, in the GO and NO-GO condition. Note that the time course of the effective connectivity between the two same units differs between the two conditions, whereas no modulation is observed in the mean PSTHs (pink) flat histograms represented along the two unit-related axes.

imposed by the behavioral task; for instance, by manipulating differentially the shared attention between different sensory modalities and the occurrence of a reward. During this Ernst Strüngmann Forum, some experts expressed the strong expectation that coordination requires an internalized supervisor or executive agent associated with a well-defined computation or function, whereas others considered that a sufficient condition might be the genesis of a symmetry-breaking of activity within the network, whatever its substrate. In this latter condition, the assembly cooperativity defines a bias or “prior” which can take forms as diverse as a propagating depolarizing wave (Chavane et al. 2000; Jancke et al. 2004; Roland 2002; Frégnac et al. 2010), local “up” states (Frégnac et al. 2006), synchrony enhancement, or frequency changes in the local field potential (LFP) spectrum (Meyrand et al. 1991; Fries 2009). In the low-level Gestalt association paradigms reviewed below, such asymmetry-breaking in cortical activity propagation takes the form of self-generated intra-VI wave which may be related to the perceptual outcome. This introductory section underlines the importance of defining further a taxonomy of coordination where the underlying mechanisms of each phenomenological form can be clearly separated (see also Moser et al. and Engel et al., this volume).

Measuring Network Coordination at a Single Recording Site

One often posits that simultaneous multiple recordings in different sites are required to track coordination (Wolf Singer, pers. comm.), and this condition becomes a necessity when coordination is engaged between processes operating simultaneously in several distant cortical areas. However, single-site recordings provide meaningful relational information, as long as the electrophysiological signal itself includes a measure of local network activity, integrated across a sufficiently wide range of space and time constants. LFP studies show that one recording site is enough to detect oscillatory synchronized activity. For instance, gamma chattering (30–80 Hz) in V1 is present in most LFP recordings during visual stimulation, whereas the probability of detecting it at the single-unit extracellular recording level remains very low, at least in the anesthetized animal (Frégnac 1991).

Another experimental strategy, reviewed in greater depth here, uses the intracellular membrane fluctuations of a single neuron as a readout probe of the correlation structure of the network afferent to the recorded cell (Figure 12.5). Intracellular recording of neocortical neurons provides a unique opportunity to characterize some statistical signature of the synaptic bombardment to which it is submitted. Indeed, the membrane potential (V_m) displays intense noise-like fluctuations, which reflect the cumulative impact arising from the coordinated activity of thousands of input neurons. It has an advantage over LFP in that the selection of the recorded assembly is not based on the distance relative to the recording site (the “visibility radius” of the LFP electrode is estimated to

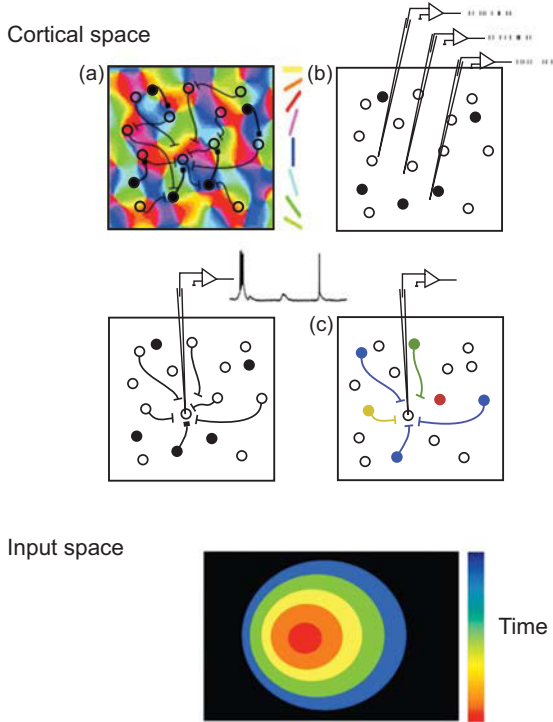


Figure 12.5 Network dynamics imaging versus synaptic functional imaging. Three methods for visualizing network dynamics are compared: (a) Optical functional imaging allows charting of cortical domains of iso-functional preference (color coded) on the basis of metabolic or hemodynamic signals. (b) Multiple simultaneous extracellular recordings are used to evaluate correlated activity patterns through the blind selection of potentially interconnected neurons. (c) The reverse analysis of subthreshold activity during long duration intracellular recordings of the same single cell can be used to retrieve the effective network afferent to the recorded cell (see text).

be 250 μm ; Nauhaus et al. 2009) but is realized by the target cell itself, which anatomically “selects” its input lines. By analyzing these fluctuations, preferably in voltage clamp mode, it should be possible to “decode” in a reverse way the global afferent activity of the network in which the cell is embedded. Despite the inherent difficulty of space clamping *in vivo* (Spruston et al. 1993), it is likely that the input lines that will be seen are the ones which have an effective impact at the soma (where the recording is done most often) and hence influence the spiking process.

For the past 15 years, we have been developing a reverse engineering approach in current clamp (Bringuier et al. 1997; Bringuier et al. 1999; Frégnac and Bringuier 1996; Frégnac et al. 2010) and voltage clamp modes (Monier et al. 2003) which allows, in principle, the retrieval of the effective connection graph in which the cell is embedded at any point in time (Figure 12.5).

The analysis is based on the synaptic rumor recorded in a single cell. Its principle is similar to that of echography in the etymological sense (transcription of echoes) and is referred to as “functional synaptic imaging” (Frégnac and Bringuier 1996). During sensory activation, the cortex is considered as a chamber of echoes produced by the thalamocortical input. The readout of the sources is based on the extraction of correlations in space and time of synaptic events with specific features of the stimulus (e.g., orientation, direction, ocular dominance). This method is equivalent to the principle of time reversal mirrors in acoustic physics and medicine (Fink 1996). The success of this demultiplexing computation relies on the underlying assumption that the input sources are separable in space and their synaptic influence travels in time with similar speed. This condition is rarely met in the general case, but seems to be valid for sparse stimulation regimes or during ongoing activity. Functional synaptic imaging gives a prediction of the macroscopic activation of the network in space and time, which can be confronted with the direct observation of the spatiotemporal cortical dynamics evoked in the superficial layers of cortex, using voltage-sensitive dyes (VSDs) (Frégnac et al. 2010).

A variety of spectral analysis methods can be applied to measure the impact of stimulus-driven coordination on the synchrony state of the synaptic bombardment afferent to the recorded cell, which can change over different time-scales, ranging from phasic (few milliseconds) to steady state (maintained for several seconds). Here we wish to underline two methods that have been used successfully to demonstrate a dependency of the cortical intracellular “hum” with the input statistics.

The first method, time-frequency wavelet analysis, has been applied with great success to reveal the stimulus-locked and stimulus-induced (which may vary in phase between trials) synchrony and oscillatory structure of assembly spiking patterns (Tallon-Baudry and Bertrand 1999; Tallon-Baudry, this volume). It provides an efficient means of achieving a trial-by-trial time-frequency analysis of the signal, at any temporal delay following stimulus onset, through an array of temporal (Gabor or Fourier) wavelets ranging from 1 to several hundred Hz (Varela et al. 2001). For intracellularly recorded cells, this multiscale filtering method can also be applied to both its supra- and sub-threshold activity (Vm) by considering an array (see raster in Figure 12.6a) of repeated responses of the same unit for different trials, precisely realigned with the stimulus onset. By using signal-noise (SNR) measures (Croner et al. 1993), highly reliable stimulus-locked events are revealed by the time-frequency SNR matrix of the subthreshold activity. These events are seen as hot peaks (Figure 12.6a) which straddle from low (wide band) to high (thin band) frequencies. In the chosen illustration, they indicate the dense presence, since repeated at many discrete times, of synchronous volleys of synaptic inputs despite a sparse postsynaptic discharge. This technique shows that the precision of time coding in V1 is dependent on the dimensionality of the stimulus. Reliability is poor for low-dimensional stimuli whereas the afferent network shows a highly

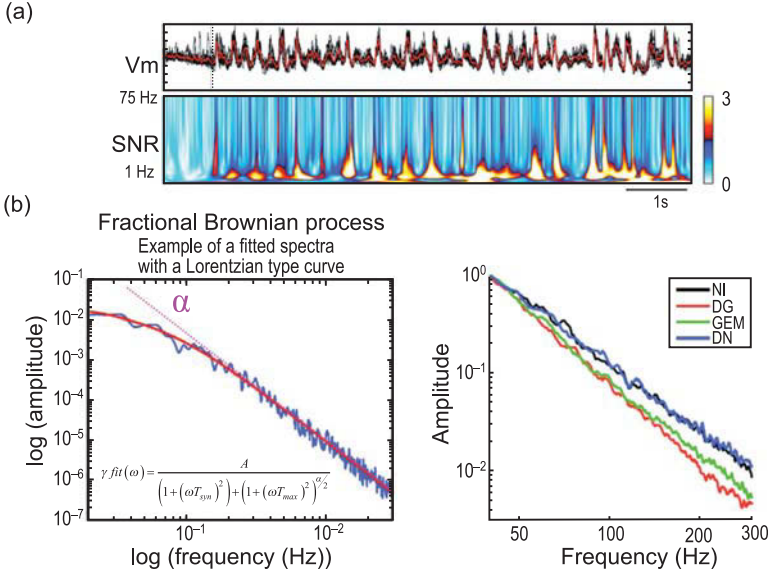


Figure 12.6 Read-out of synaptic input coordination in a single V1 neuron using time-frequency and spectral fractal analysis. (a) Synaptic input coordination measured by wavelet analysis of subthreshold intracellular dynamics. Top panel: trial-by-trial membrane potential trajectories are overlaid in black; in red, mean Vm response. Lower panel: time-frequency wavelet analysis of the Vm dynamics and signal-to-noise (SNR) power matrix in a V1 Simple cell (Frégnac et al. 2005; Baudot et al., submitted). The time axis represents 400 ms of ongoing activity followed by several seconds of continuous visual activation with a pseudorandom animation (kept identical across trials) of natural scenes. The colored SNR peaks straddling between 1–75 Hz signal the reliability of the evoked synaptic bombardment and the presence of highly temporally structured input when processing natural scenes. (b) Extracting the contextual network correlation state from the spectral properties of the membrane potential of a single cell. Left: scaling invariance of the power law for a Lorentzian process and asymptotic linear fall-off (slope α) in a log-log coordinate plot. Same analysis applied to the subthreshold dynamics of a single V1 cell for various input statistics (DG: drifting grating; GEM: grating with eye movements; NI: natural image; DN: dense noise). The fractal slope component shows a strong stimulus dependency in the coordination effectiveness of the network activity “seen” by the recorded cell (adapted from El Boustani et al. 2009).

structured input for natural scene statistics (Frégnac et al. 2005; Marre et al. 2005; Baudot et al., submitted).

The power spectrum of the membrane potential of any given cell provides another valuable tool to extract information on the second order statistics of the synaptic input bombardment. A recent study from our lab has demonstrated that the power spectral density of the subthreshold membrane potential (Vm) of visual cortical neurons can be fitted by a power function $1/f^\alpha$, at least in the upper temporal frequency range between 80–200 Hz (El Boustani et al. 2009). This observation holds both during ongoing activity and evoked states, although the power law slope changes as a function of input statistics: the fractional

exponent α is given by the fall-off slope of the Vm spectrum in a log-log representation and provides a measure proportional to the range of the temporal correlations (the larger the longer). The linear asymptotic behavior of the log-log plot, called power law scaling, is shared by many complex dynamic or self-organizing processes, both in physics and biology. The origin of their shape invariance with frequency rescaling ($f \rightarrow kf$) is a matter of debate for multiple recordings of LFPs and spiking assemblies (Beggs and Plenz 2003; Plenz and Thiagarajan 2007). Until recently, it was thought that the slope component was dominated by the intrinsic conductance repertoire of the cells (Bedard and Destexhe 2008). *In vivo* recordings from our lab show that the fractional slope component value varies with the complexity of the sensory input statistics (El Boustani et al. 2009; see Figure 12.6b) and that the short-range correlations present during natural scene viewing are of the same range as those found in ongoing activity. These results have been emulated by computational models, which demonstrate that the fractional exponent is determined by the mean level of correlation imposed in the recurrent network activity. Similar relationships have also been reproduced in cortical neurons recorded *in vitro* with artificial synaptic inputs by controlling *in computo* the level of correlation in real time (using dynamic clamp techniques). From this confrontation between theory and electrophysiological recordings, we conclude that the frequency-scaling exponent of subthreshold Vm dynamics provides a reliable measure to monitor changes in the coordination state of neural networks, when they are maintained for several seconds or longer. This multiscale analysis could be potentially generalized with other types of signals which achieve integration of neural activity at more meso- or macroscopic scales.

Reconstruction of Lateral Propagation Waves from Synaptic Echoes

The combination of intracellular electrophysiology and VSD network imaging in the study of visual cortical processing has given unprecedented access to binding and coordinating processes that operate at a subthreshold level, and which cannot be detected by solely studying spiking activity. These techniques give evidence for propagation along long intracortical distances of depolarizing waves, which may contribute to facilitate synaptic integration anisotropically in the cortical network. On one hand, VSD imaging reveals the spatio-temporal signature of information propagation across the target network, and reflects anatomical constraints in the “divergence” of the connectivity. On the other, intracellular recordings characterize the “convergence” of the connectivity to any given cortical locus. They provide evidence that the receptive field of visual cortical neurons is not limited to a tubular view but extends over a large region of the visual field. The mean discharge field (MDF) size of V1 cells defines a spiking receptive area that does not extend beyond 1–2 degrees

of visual angle for vision around the area centralis in the cat (the equivalent of our fovea). In contrast, the synaptic integration field, reconstructed from intracellular recordings, corresponds to the region of space from which a local input still evokes a significant excitatory or inhibitory response. It captures synaptic echoes that originate from the far “silent” surround of the classical discharge field (Figure 12.7). Schematically, the subthreshold receptive field is characterized by a hill of spatial sensitivity (falling off 5–10° away from the MDF center) and a basin of latency: synaptic responses elicited by stimuli placed far from the center of the discharge field show increasing delays (up to several tens of milliseconds) with the relative eccentricity (Bringuier et al. 1999).

Functional synaptic imaging offers a link between these two modes of visualization of apparently distinct connectivities (“divergence” vs. “convergence”): although our method is based only on inferences established from intracellular records, it allows the reconstruction—first in space, then in cortex—of the source location distribution corresponding to the recorded synaptic echoes produced by the sensory drive. The hypothesis of a traveling wave is made on the assumption of symmetry in exuberant intrinsic connectivity: since

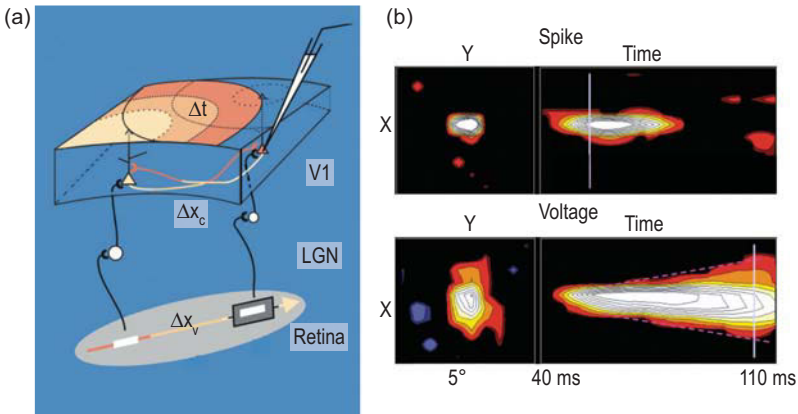


Figure 12.7 Functional synaptic imaging. (a) Schematic representation of the hypothesis of reciprocal horizontal connections between two cortical cells (left, “sender”; right “receiver”). This schema allows reconstruction of a propagating wave (circles) from the intracellular measure of evoked latencies of synaptic responses in the “receiver” cell (right, electrode). Δx_v is the eccentricity of the distal stimulus (white rectangle, no outline) from the central stimulus shown in the discharge field center (grey rectangle, black outline). Δt is the latency between the synaptic response onsets evoked through the two pathways. Δx_c is the intracortical distance between the cortical feedforward impacts produced by the two stimuli, inferred from the known retinocortical magnification factor (see text for details). (b) Spatiotemporal (left: X–Y; right: X–t) maps of supra-threshold (spike, upper panels) and subthreshold (voltage, lower panels) activations in the same V1 cell. The X–Y maps are presented for two specific delays corresponding, respectively, to the maximal extents of the discharge field (upper) and subthreshold integration field (lower). The pink dotted lines show the average speed of the propagation of the reconstructed wave ($0.2\text{--}0.4\text{ m s}^{-1}$) (adapted from Frégnac et al. 2010).

V1 is a highly recurrent network, we assume that each cell is connected reciprocally to any other cell, with identical propagation delays from and to the cell (Figure 12.7a). In simpler terms, it should take exactly the same amount of time for any given cell to receive a signal from a distant cortical source as to send it back to the same cortical locus. This theoretical shortcut allows the inference of propagation patterns (the cell being seen as a “wave emitter”) solely on the basis of the spatiotemporal maps of stimulus-locked synaptic responses recorded in a single cell (the cell being seen as an “echo receiver”). As illustrated in Figure 12.7b, the slopes (dotted lines) seen in the spatiotemporal pattern (X-t) associated with the receptive field (X-Y) corresponds to the subthreshold latency basin of the recorded cell (Binguier et al. 1999). This suggests that the information received from the receptive field center in the cortex through the feedforward afferents is then propagated radially by the horizontal connectivity to neighboring regions of the visual cortex over a distance that may correspond to up to 10 degrees of visual angle. These data led successfully to the functional identification and reconstruction of a propagating wave of visual activity relayed by the horizontal connectivity.

The principle of computation of the propagation speed from the intracellular recording is straightforward (Figure 12.7a): we compare the synaptic effects of two elementary stimuli (white bar), one in the core of the minimal discharge field, the other in the “silent” surround. The distance between the primary points of the feedforward impact produced in cortex by the two stimuli can be predicted on the basis of their relative retinal eccentricity Δx_v and the value of the retino-cortical magnification factor (RCMF). This factor can be measured electrophysiologically in cat (Albus 1975), by 2-deoxyglucose metabolic labeling in monkey (Tootell et al. 1982), by intrinsic imaging in mouse (Kalatsky and Stryker 2003), and even by fMRI in humans (Warnking et al. 2002). Thus, beyond a certain scale of spatial integration (larger than the columnar grain), any distance in visual space, Δx_v , can be converted to a distance in visual cortex, Δx_c . The spatial range of the subthreshold field extent agrees with the anatomical description of 4–7 mm horizontal axons running across superficial layers in cat V1 (Mitchison and Crick 1982). Although the RCMF factor is dependent on the eccentricity from the fovea in primates and humans, this is not the case in cats and ferrets, where 1° of visual angle corresponds roughly to 1 mm in cortex within the 10° of the area centralis. Furthermore, the electrophysiological recordings give access to the delay Δt_c between the two synaptic echoes obtained through the feedforward and the horizontally mediated pathways. By dividing the inferred cortical distance Δx_c in cortex by the recorded delay Δt_c , an apparent horizontal propagation speed can be computed within the cortical map, hence in the plane of the layers of V1. The propagation speeds we inferred range from 0.02–2 m s⁻¹, with a peak between 0.1–0.3 m s⁻¹.

These velocity values have since been confirmed for other sensory cortical structures, such as somatosensory cortex (Moore and Nelson 1998). They are

thus ten times slower than X-type thalamic axonal propagation and feedback from higher cortical areas (2 m s^{-1} ; Nowak and Bullier 1997) and one hundred times slower than the fast Y-pathway ($8\text{--}40 \text{ m s}^{-1}$; Hoffman and Stone 1971). They are, in fact, within the order of magnitude of conduction speeds measured *in vitro* and *in vivo* along nonmyelinated horizontal cortical axon fibers. In view of the difference in size that exists between the subthreshold receptive field and the discharge field, propagation most likely involves long monosynaptic horizontal connections, although the contribution of rolling waves of postsynaptic activity cannot be entirely excluded. Recent reports based on cortical LFPs triggered on LGN spike activity rule out the possibility that divergence of LGN axons may also contribute to the buildup of the observed latency shifts as discussed by Nauhaus et al. (2009).

Thus, our intracellular study of synaptic echoes detects the propagation signature of an intracortical wave of visual activation traveling along long-distance horizontal connections. One obvious consequence is that the V1 network should not be considered as an ordered mosaic of independent “tubular” analyzers, but rather as a constellation of wide field integrators, which simultaneously integrate input sources that arise from much larger regions of visual space than previously thought. The collective behavior of these integrators is coordinated during sensory processing by the anisotropic propagation of stimulus-induced facilitatory waves traveling at slow speed within the superficial cortical layers. Primary visual cortical neurons thus would have the capacity to combine information issuing from different points of the visual field, in a spatiotemporal reference frame centered on the discharge field itself. This ability imposes precise constraints in time and in space on the efficacy of the summation process of elementary synaptic responses, and specific functional predictions linked to the intracortical genesis of coordinating waves will be reviewed below.

The macroscopic reconstruction of intra-V1 waves on the basis of microscopic echoes remains, however, an extrapolation made between two scales of spatial organization differing by two orders of magnitude (neuron vs. map). Brain imaging methods, and more specifically VSD techniques, give an unprecedented view of the state of the cortical network, best detected as a depolarizing field in the terminal tuft of the dendrites of layer 2/3 pyramidal cells (Roland 2002), with a time sensitivity close to that of intracellular recordings. Since the pioneering study of cortical spread function by the group of Amiram Grinvald (1994), numerous groups have confirmed the propagation of spontaneous and evoked waves across the cortical laminar planes in visual primary and secondary cortical areas of rodents and higher mammals: rat, from $0.05\text{--}0.07 \text{ m s}^{-1}$ (Xu et al. 2007); cat, 0.09 m s^{-1} (Jancke et al. 2004); cat, 0.3 m s^{-1} (Benucci et al. 2007); monkey: 0.20 m s^{-1} (Grinvald et al. 1994).

The group of Matteo Carandini measured, in both cat and monkey V1, the spatial distribution and the temporal phase of the second harmonic VSD response to the contrast reversal of a one-dimensional bar (Benucci et al. 2007).

The spatial spread attenuation constant of the cortical response was found to correspond quantitatively, in each species studied, to the mean extent of horizontal axons (2–3 mm in monkey, 5–8 mm in cat). The response phase (i.e., the temporal delay of the evoked oscillation in each pixel with respect to the inducer stimulus) was shown to increase linearly as a function of the lateral distance from the feedforward impact zone of the bar. These observations, which have since been replicated by LFP studies applied to multielectrode grid recordings (Nauhaus et al. 2009), confirm that the focal stimulus induced a traveling wave across cortex, with an apparent speed of propagation estimated at around 0.30 m s^{-1} . As shown in Figure 12.8, these VSD studies fully corroborate the predictions we extracted from our intracellular recordings more than ten years ago (Bringuier et al. 1999), and most remarkably both methods

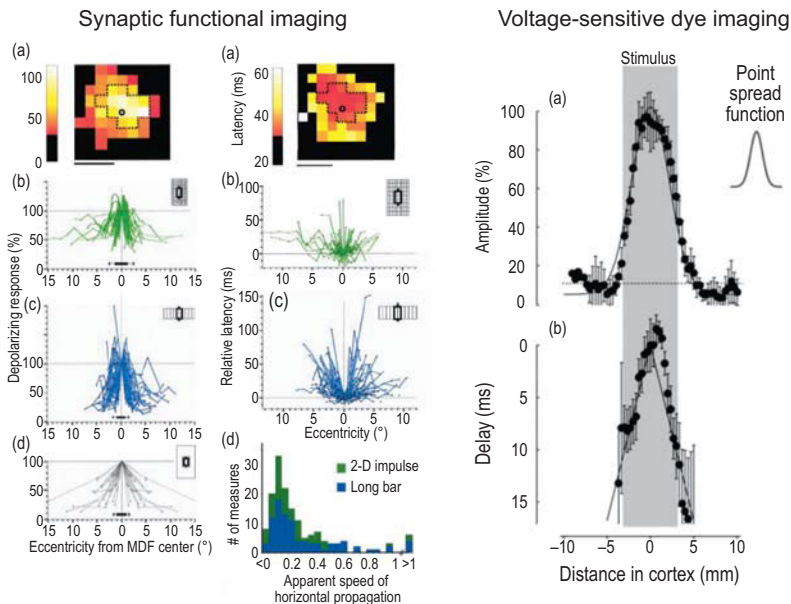


Figure 12.8 Comparison of spatial and temporal properties of horizontal propagation, using synaptic functional imaging (left) and network voltage-sensitive dye (VSD) imaging (right). See text for details. Synaptic functional imaging is used to infer propagation waves from the readout of synaptic echoes recorded in the same single cell in response to sparse localized inputs. VSD imaging monitors the cortical lateral spread of a depolarizing wave triggered by an ultrathin phase reversed contrast grating. Left panel: horizontal propagation inferred with intracellular synaptic functional imaging (adapted from Bringuier et al. 1999). Right panel: horizontal propagation wave monitored in the superficial layers of cat V1 with the f_2 component of the VSD imaging signal (adapted from Benucci et al. 2007). Note the similarities between the spatial hill sensitivity profiles (left column) obtained with intracellular recordings and with VSD imaging (top right panel). The same propagation speed ($0.1\text{--}0.3 \text{ m s}^{-1}$) is measured by the two imaging techniques (second column from the left and bottom right panels).

give the same mean estimate of propagation speed (0.30 m s^{-1}) although they are based on different measurement methods and analysis. As nicely worded by Nauhaus (2009:72), one may conclude with some confidence that “the synaptic input to neurons during spontaneous activity can be thought of as the superposition of a myriad of traveling waves originating from individual spikes distributed over an extended region of cortex.”

Visualizing Correlates of Gestalt Illusions in V1

The multiscale comparison of these various different imaging techniques (synaptic functional imaging, VSD network imaging) opens up a new field of study, where it becomes possible to compare real-time imaging in cortical networks with membrane dynamic recording in single cells, on the one hand, and psychophysical performance measures, on the other. Almost a century ago, psychologists and philosophers proposed a theory of perceptual grouping, Gestalt (Koffka 1935; Köhler 1947), which predicts the emergence of coherent percepts of global shape and motion from the temporal superposition of static presentations of elementary spatial features. This theory assumes the existence of psychic processes that favor associations in space (according to spatial proximity and similarity in contrast polarity) as well as in time (continuity, common fate).

Those predictions inspired a series of psychophysical studies, whose results strongly support the following working hypothesis: the temporal characteristics of the recruitment of the “horizontal” intracortical connectivity could affect the perception of motion. Among various demonstrators, the “Phi” apparent motion protocol, originally called the “beta phenomenon” by Wertheimer (1912), induces a powerful illusion when the same target is repeatedly flashed at different moments in time in different positions in the visual field ordered along an imaginary trajectory (Figure 12.9, left). Although at each moment in time the observer sees only a static image, he reports the perception of continuous motion of the same object along the trajectory defined by the “association” path linking the various positions explored in succession. The strength of the percept depends on the complexity of the test stimulus (shape and texture), the duration of the static presentations, the interstimulus interval, and the spatial offset between positions (Anstis et al. 1998). The “line motion” illusion is also based on the same induction process of asynchronous static presentations. In this latter case, the cue feature is a uniform luminance square, followed by a bar of the same luminance, one polar end of which encroaches on the previously flashed square. For adequate interstimulus intervals and presentation durations, the human subject reports a continuous movement of one border, perceived as a smooth morphing of the square into the elongated bar (Hikosaka et al. 1993).

If the spatial contextual effect can be easily interpreted in the framework of the perceptual “association field” of Field et al. (1993), the temporal

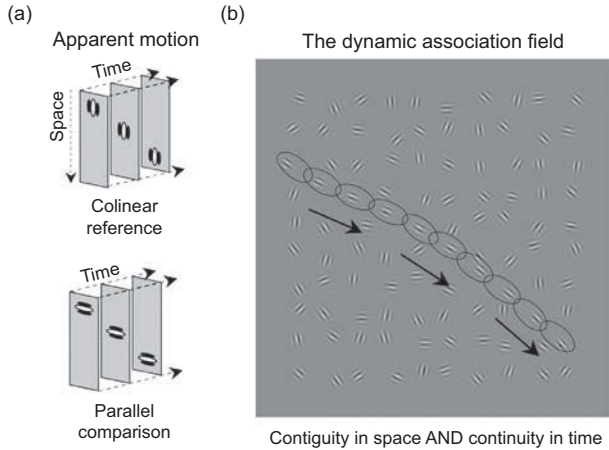


Figure 12.9 Apparent motion and the hypothesis of the “dynamic association field.” (a) Two forced-choice apparent motion protocol, where the human observer has to report which sequence of oriented elements is seen “faster.” Two configurations are compared (collinear and parallel), in which the orientation of each element is respectively collinear or orthogonal to the downward motion axis. (b) The “dynamic association field” hypothesis. Local oriented inputs (Gabor patches) induce a facilitation wave of activity traveling along horizontal connections intra-V1. This wave binds in space and time proximal receptive fields with co-linear preferred orientations, thus creating a contiguous path of temporal integration. The associative strength of the perceptual effect is maximal when the asynchronous feedforward sequence produced by joint strokes of apparent motion (arrow) travels in phase in the cortical network with the visually evoked horizontal propagation.

determinants and the preferred co-linearity configuration of these effects suggest a strong dependency on the intra-V1 horizontal connectivity and its propagation speed constraint. VSD imaging correlates of the “line-motion” illusion have been found in area 18 of the anesthetized cat (Jancke et al. 2004). Grinvald’s team compared the spatiotemporal patterns of the cortical responses to a flashed small square and a long bar alone, and the configuration of the line-motion illusion: a square briefly preceding by a few tens of milliseconds the presentation of a light bar (co-linear with the square). In the (last) associative condition, the VSD pattern demonstrated the spread of a low-amplitude wave in the cortical layer plane, extending far beyond the retinotopic representation of the initial “cue.” This spread was most visible along the main orientation axis of the bar, with a horizontal propagation speed around 0.10 m s^{-1} . This pattern was indistinguishable from the spatiotemporal pattern produced by the continuous motion of the same square at a few tens of degrees per second. Thus, most remarkably, the anisotropic spread of the cortical activity pattern relayed by the horizontal connectivity observed in primary visual areas was isomorphic to the percept of the continuous square-bar morphing reported by the human observer.

Visualizing Propagation of Orientation Belief

An important issue in our understanding of coordination in sensory cortical areas during low-level perception is to determine how much of the perceptual biases results from structural built-in constraints and how much derives from contextual activity or coordination effects defined by the stimulus configuration itself. For instance, psychophysical studies show that a two-stroke flashed sequence of oriented elements displaced along their orientation axis appears to move “faster” to human observers than the same stimulus sequence at an angle to the motion axis. This effect peaks at $64^\circ/\text{s}$ in humans and decreases for higher and lower speeds (Georges et al. 2002). This speedup is highly sensitive to orientation anisotropy, strongly depends on the relative angle between the orientation of the moving elements and the motion axis, and is still observed for curvilinear trajectories. This suggests that it involves units highly sensitive to orientation, a property mainly expressed by neurons in areas V1 and V2. Two features of the perceptual effect are closely related to V1 physiology and anatomy: (a) the sensitivity of the speedup effect to orientation resembles that of the recently uncovered “association field” (Field et al. 1993) presumably involved in contour integration; (b) the speed at which the speedup is maximum is comparable to the speed at which neural activity propagates along long-range horizontal connections. This structure–perception match may be adapted to a specific oculomotor exploration strategy since the conversion of the horizontal propagation speed in degrees of visual angle per second in the visual field (which depends on the species-specific cortical magnification factor) corresponds in most species to the saccadic range of eye movements ($50\text{--}500^\circ/\text{s}$).

As stated above, it is generally assumed that orientation binding results from anisotropies in the intracortical connectivity, where long-distance horizontal axons in visual cortex have been reported to link columns sharing similar orientation preference. However, the anatomical evidence in favor of such bias is rather scarce in the cat cortex (the strongest evidence for a structure–function correlation has been obtained in the tupaia glis and the ferret V1). Combinations of optical imaging and intracellular labeling show indeed a diversity of potential links established between orientation columns which do not obey, at least at the statistical significance level, the rule “like couples to like” (Monier et al. 2003). Quantitative reanalysis of published data correlating axonal bouton distribution with target orientation preference (relative to that of the parent cell) revealed by intrinsic imaging reveals that the tendency for horizontal axons to connect iso-orientation loci is not exclusive and interconnection probability is only about 1.5 times greater than chance level. This bias has been mostly observed for supralaminar pyramidal neurons. However, inhibitory interneurons and neurons in layer IV or close to pinwheel centers have also been reported to connect lateral orientation columns in a cross-oriented or unselective way (Karube and Kisvarday, pers. comm.). As a consequence, at a more integrated mesoscopic level, the net functional effect cannot be predicted.

From "Dynamic Coordination in the Brain: From Neurons to Mind,"

C. von der Malsburg, W. A. Phillips, and W. Singer, eds. 2010. Strüngmann Forum Report, vol. 5, series ed. J. Lupp. Cambridge, MA: MIT Press. ISBN 978-0-262-01471-7.

Other processes, such as activity-driven coordination, may amplify a small structural bias in a strong perceptual effect, when enough temporal synergy and spatial summation are recruited from the start by the sensory drive. A recent collaborative work between our lab and the group of Amiram Grinvald attempted to achieve a multiscale analysis of the visually driven horizontal network activation, using population and single-cell measures of postsynaptic integration. VSD imaging showed that a local-oriented stimulus evoked an orientation-selective activity component that remained confined to the feed-forward cortical imprint of the stimulus. Orientation selectivity decreased exponentially along the horizontal spread (space constant ~ 1 mm). To dissect the local connectivity rules, we also made intracellular recordings during dense-oriented Gabor noise stimulation to identify the orientation selectivity and preference of converging horizontal inputs onto the same target cell. The combination of the imaging and electrophysiological results suggests, somewhat surprisingly, that the horizontal connectivity does not obey iso-orientation rules beyond the hypercolumn scale. In contrast, when increasing spatial and temporal summation, both optical imaging and intracellular measurements showed the emergence of an iso-orientation selective spread. We conclude that stimulus-induced cooperativity is a necessary constraint for the emergence of iso-functional Gestalt-like binding (Chavane et al., submitted).

This last study, combining network VSD imaging and synaptic functional imaging, shows two contrasted dynamic behaviors of the same network for two distinct levels of coordination driven by the stimulus configurations: a single local stimulus does not propagate orientation preference through the long-range horizontal cortical connections whereas stimulation imposing spatial summation and temporal coherence facilitates the buildup of orientation preference propagation. These observations do not forcibly contradict each other. On one hand, for the local-oriented stimulus, the divergent connectivity pattern may facilitate detection of high-order topological properties (e.g., orientation discontinuities, corners, geons). On the other hand, for stimulation protocols involving a larger extent of stimulation, summation of multiple-oriented sources in the far “silent” surround can optimize the emergence of iso-orientation preference links. Configurations such as oriented annular stimuli may, for instance, recruit iso-oriented sources collinearly organized with the orientation preference axis of the target column/cell; similar synergy may be obtained when sources, independent of their exact location, share the same motion direction sensitivity as the target grating. Both of these configurations, which are confounded in annular aperture protocols, correspond to the neural implementation of the Gestalt’s continuity and common fate principles, but other more dynamical principles could also emerge from such network configuration.

These different experimental observations have led us to formulate the concept of the “dynamic association field” (Frégnac et al. 2010), which adds a temporal coordination dimension to the static “association field” introduced originally by Hess and Field (Field et al. 1993). In its dynamic version, the

revised concept assumes that local-oriented inputs (Gabor patches) induce a facilitation wave of activity traveling along horizontal connections intra-V1 (Figure 12.9a). This coordination wave tends to bind proximal receptive fields with co-linear preferred orientations, thus creating a contiguous path of temporal integration. The associative strength of the perceptual effect is maximal when the asynchronous feedforward sequence produced by joint strokes of apparent motion (arrow in Figure 12.9b) travels in phase with the visually evoked horizontal intracortical propagation. Several arguments strongly support the relevance of introducing a time coordination. Intracellular recordings show that centripetal apparent motion produced by iso-oriented Gabor stimuli (co-aligned with the motion axis and presented from periphery to center) at saccadic speed ($250^\circ/\text{sec}$ in the cat) is more efficient than the simultaneous static presentation of the same stimuli (or the reverse centrifugal sequence) at evoking subthreshold synaptic responses from the “silent” periphery. Recent unpublished intracellular work from our lab shows that sparse apparent motion two-stroke noise appears as a powerful stimulus condition to trigger the coordination of synaptic activity along motion streaks attuned to the orientation preference of the target cells (Carelli, Pananceau, Monier, and Frégnac, in preparation).

Conclusion

The coordination processes that we have reviewed are generated mostly by recurrent and lateral intrinsic connections in the same cortical area, with a possible contribution of feedback control from higher cortical areas (although it may be minored by deep anesthesia). In terms of cognition/perception relevance, these processes are low level and not linked to attention since they are observed in humans during forced choice tasks as well as in the anesthetized mammal. These various interdisciplinary studies, based on intracellular electrophysiology, network imaging, and psychophysics, all point to the emergence of cooperative Gestalt-like interactions, when the stimulus carries a sufficient level of spatial and temporal coherence. Above a given activation threshold (yet to be quantitatively defined), a cooperative depolarizing or facilitatory wave becomes detectable in primary and secondary visual areas. The trigger zone can be considered as the initial point in cortical space where the symmetry of the compound effect of neural activity creates symmetry-breaking (see Engel et al., this volume). This process, which can occur spontaneously or be evoked during sparse sensory stimulation regime, initiates a wave that travels at low speed in the plane of the superficial cortical layers ($0.10\text{--}0.30\text{ m s}^{-1}$) and most likely becomes anisotropic for oriented inducer stimuli. The physiological features of the spatiotemporal propagation–coordination pattern recorded in V1 are highly correlated with the percept reported by the conscious human observer (e.g., Georges et al. 2002) and agree with predictions derived

from the Gestalt theory. In the two cases of motion illusion reviewed here (apparent motion and line motion), a wave of perceptual binding modulates the integration of feedforward inputs yet to come: this wave can be seen as the propagation of the network belief of the possible presence of a global percept (the “whole”: here, continuous motion of a space-invariant shape) before the illusory percept becomes validated by the sequential presentation of the “parts” (signaled by direct focal feedforward waves). This neuronal dynamics obeys closely the Gestalt prediction that the emergence of the “whole” should precede in time the detection of the “parts.”

These cortical processes result, at the perceptual level, in the propagation of functional biases binding of contour and motion, which goes beyond the scale of the columnar orientation and ocular dominance network. It remains to be determined whether the correlations we report between perception and horizontal propagation are the sole result of neural processes intrinsic to V1, or whether they reflect the reverberation in V1 of a collective feedback originating from multiple secondary cortical areas, each encoding for a distinct functional representation of the visual field. It may be indeed envisioned that the primary visual cortex plays the role of a generalized echo chamber fed by other cortical areas (visual or not) that participates in the coding of shape and motion in space: accordingly, the waves traveling across V1 would signal the emergence of perceptual coherence when a synergy is reached between the different cortical analyzers. Synaptic functional imaging provides a new way to explore the genesis and propagation of such slow coordination, which may be instrumental to low-level cortical-mediated cognition.

Acknowledgments

This work has been supported by the CNRS, and grants from the French ANR and the European Community (FACETS (FET- Bio-I3: 015879) and BRAIN-I-NETS (FET-Open: 243914).